ACS Biomaterials SCIENCE & ENGINEERING

Open Access
This article is licensed under CC-BY-NC-ND 4.0

pubs.acs.org/journal/abseba
Article

Assessment of Bovine Collagen Manufactured via Cellular Agriculture

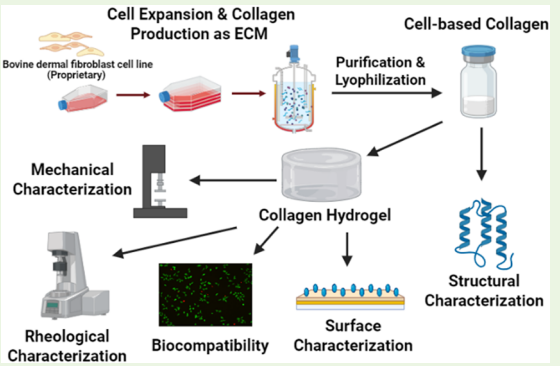
Nafi Ahmed, Corbin M. Goodwin, Megan Hales, Juan Camacho, Christopher Gilchrist, and Rohan A. Shirwaiker*

Cite This: ACS Biomater. Sci. Eng. 2026, 12, 3177−3187

Read Online

ACCESS | Metrics & More | Article Recommendations

ABSTRACT: Cellular agriculture offers a transformative approach to protein production by creating biologically derived alternatives to animal-sourced biomaterials. This study focuses on the comprehensive characterization of bovine collagen produced via cellular agriculture. A bovine fibroblast cell line optimized for collagen production was cultured in a custom bioreactor system to produce collagen (≥95% type I), which was extracted, purified, lyophilized, reconstituted at 8 mg/mL, and cast into self-assembling fibrillar hydrogels (Ø8 × 4 mm^2) at neutral pH and 37 °C. Functional properties of this cell-based (CB) collagen were benchmarked against traditional animal-derived (AD) bovine collagen. SDS-PAGE confirmed their molecular similarity, revealing characteristic α-chains (∼120 kDa), β-dimers (∼240 kDa), and γ-trimers (∼300 kDa). Amino acid analysis showed nearly identical amino acid profiles, and differential scanning calorimetry analysis highlighted equivalent thermal stability between them. Furthermore, circular dichroism spectroscopy confirmed preservation of the triple-helical structure in the CB collagen. Mechanical testing demonstrated that CB hydrogels possessed significantly higher compressive and dynamic moduli (1260 ± 191 Pa and 6250 ± 1031 Pa, respectively) compared to the AD hydrogels (890 ± 255 Pa and 3134 ± 1857 Pa, respectively) ($p < 0.05$), indicating better structural integrity and shape retention. Rheological analysis supported these findings, indicated by the higher storage and loss moduli of CB hydrogels (48.40 ± 8.5 Pa and 13.20 ± 1.3 Pa, respectively) than AD hydrogels (25 ± 2.12 Pa and 10 ± 1.58 Pa, respectively) ($p < 0.05$). Surface wettability testing highlighted comparable hydrophilicity for CB and AD collagens. Finally, the biocompatibility of the CB hydrogels was evident from the notable increase in cultured fibroblast cell density, live cell area, and metabolic activity over 7 days. This comparative assessment underscores the functional equivalence of CB collagen with conventional animal-derived sources and offers critical insights for optimizing cellular agriculture-based production systems and hydrogel formulations for application-specific requirements in the future.



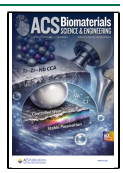
KEYWORDS: *collagen, cellular agriculture, hydrogel, cell-based, biomaterial characterization*

1. INTRODUCTION

The global demand for protein continues to grow rapidly, driven by population growth and rising affluence.[1] This includes the demand for high-quality, protein-rich biomaterials for medical and cosmetic applications as healthcare and personal care industries expand. While animal-derived protein biomaterials such as collagen have long been the standard in these industries, their production can involve challenges such as supply constraints, batch-to-batch variability, and risks of transmission of pathogens such as bovine spongiform encephalopathy.[2] Cellular agriculture offers a complementary approach that leverages cell culture technologies to produce animal-free proteins, and it can enable consistent protein quality and purity while reducing the reliance on traditional animal sources.[3]

Collagen is a versatile protein widely used in biomedical, food, and cosmetic applications due to its unique structural and functional properties. Its rheological and mechanical properties allow the formation of gels, films, scaffolds, beads, and nanoparticles.[4] Collagen, being the main structural component of the extracellular matrix (ECM), is indispensable for wound dressing, cell culture, and tissue engineering applications.[5,6] In the food industry, collagen and its derivatives, such as gelatin, are often used to enhance texture

Received: December 23, 2025
Revised: April 23, 2026
Accepted: April 24, 2026
Published: May 8, 2026



© 2026 The Authors. Published by American Chemical Society

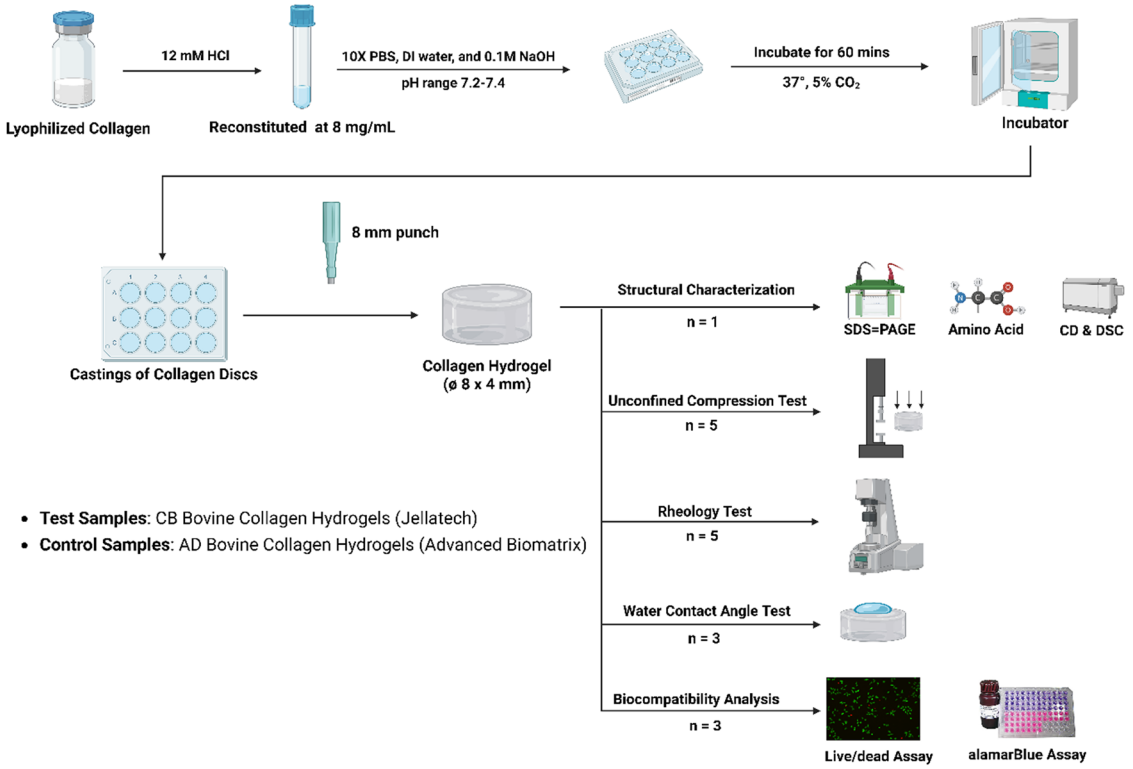


Figure 1. Schematic representation of collagen hydrogel preparation and characterization workflow. Graphics created in BioRender. Ahmed, N. (2026) https://BioRender.com/jj1791p.

and stability of food products, and as biodegradable packaging materials.[7] Collagen is typically sourced from bovine and porcine tissues, and given the aforementioned challenges, is an excellent candidate for production via cellular agriculture. Beyond its traditional applications, collagen produced via cellular agriculture can also serve as bioactive scaffolding for cell-cultivated meat, offering structural and functional properties that plant-based scaffolding cannot recapitulate.[8−10]

While microbial fermentation systems are commonly used for recombinant protein production, replicating full-length, triple-helical collagen with essential post-translational modifications, such as proline and lysine hydroxylation, remains challenging.[11,12] Recombinant collagen produced in non-mammalian systems often consists of truncated peptides or fragments that lack critical post-translational modifications and native supramolecular organization, limiting their structural fidelity and functionality.[13] Mammalian cell culture platforms can overcome these limitations by supporting such modifications, enabling the production of structurally complete collagen. In particular, collagen synthesized by mammalian fibroblasts can retain the native full-length heterotrimeric type I architecture together with the post-translational modifications required for stable triple-helix formation and fibrillogenesis.[14] While collagen biosynthesis in vitro has been widely documented, such studies have primarily focused on extracellular matrix deposition in conventional two-dimensional culture systems, typically in the context of cell biology and tissue engineering research.[15−17] In contrast, cellular agriculture platforms utilizing three-dimensional perfusion culture and downstream purification technologies can enable controlled, reproducible, animal-free production of collagen as a standalone biomaterial. Furthermore, such production platforms create opportunities for future biochemical customization, such as preservation of telopeptides through gentle extraction strategies, targeted genetic modification, or molecular tagging to tailor collagen functionality for specific applications.[18]

Despite these advances, an important question remains regarding whether collagen produced via cellular agriculture can accurately recapitulate key properties of conventional animal-derived (AD) collagen, a comparison that is currently absent in the literature. Thus, in the early phases of cellular agriculture technology development, it is important to comprehensively evaluate the physicochemical and functional equivalence of cell-based (CB) collagen relative to traditional AD sources. Accordingly, this proof-of-concept study investigates the structural, rheological, mechanical, and cell-growth characteristics of bovine CB collagen in comparison with AD collagen under identical solution and hydrogel preparation protocols and characterization conditions.

2. MATERIALS AND METHODS

Figure 1 provides an overview of the study design to characterize several key attributes essential for understanding the CB collagen's suitability, especially for biomedical and food applications. First, SDS-PAGE (sodium dodecyl sulfate-polyacrylamide gel electrophoresis) was employed to verify the molecular weight distribution, and circular dichroism spectroscopy to verify the presence of collagen's characteristic triple-helical structure. In addition, amino acid analysis and DSC analysis were conducted to compare the amino acid composition and thermal properties, respectively, of CB and AD collagen. Then, rheological testing was performed to evaluate the hydrogels' viscoelastic properties. Next, the mechanical properties of the hydrogels were determined via unconfined compression testing, and their wettability was determined using a water contact angle test. Lastly, the hydrogels' biocompatibility was assessed using a 7-day in vitro cell culture study.

https://doi.org/10.1021/acsbiomaterials.5c02203
ACS Biomater. Sci. Eng. 2026, 12, 3177−3187

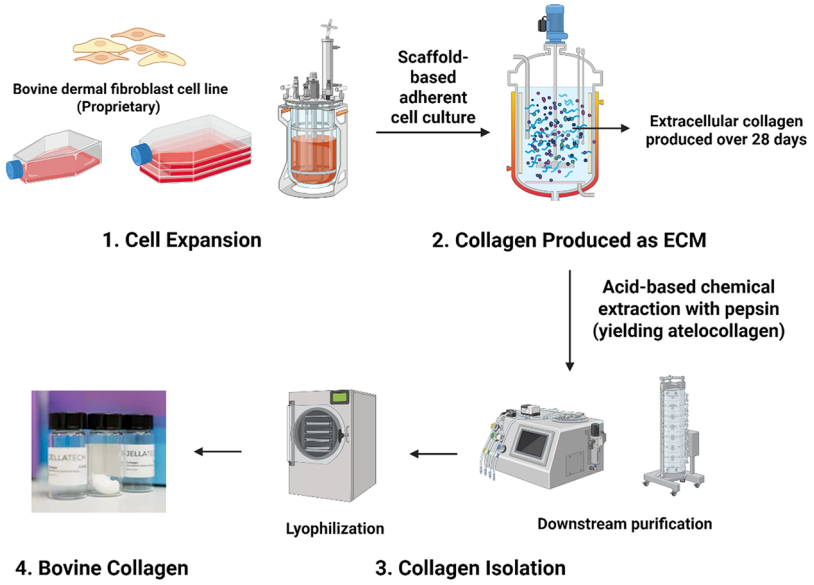


Figure 2. Overview of the CB bovine collagen production workflow. Graphics created in BioRender. Ahmed, N. (2026) https://BioRender.com/qx1y1j2.

2.1. CB Bovine Collagen Preparation

CB collagen (>95% Type I) was produced using proprietary cellular agriculture technology (Jellatech Inc., NC), an overview of which is presented in Figure 2. Briefly, collagen was generated via in vitro culture of a bovine dermal fibroblast cell line previously established by Jellatech Inc. as part of its commercial operations, independent of the present study. The adherent cells were first cultured (37 °C, 5% CO_2) in Dulbecco's Modified Eagle Medium (DMEM) supplemented with 10% fetal bovine serum (FBS) and 1% penicillin-streptomycin (Thermo Fisher Scientific, MA) in T-flasks, and upon reaching confluence, transferred to custom fixed-bed bioreactors (0.5−1L) for further expansion. Collagen secretion was induced using a proprietary stimulation protocol, allowing extracellular matrix (ECM) proteins to accumulate in the fixed-bed matrix of the bioreactor over 28 days. Afterward, atelocollagen was harvested via acid and enzymatic digestion with pepsin and purified using proprietary methods (noncollagenous material removed via chemical treatment, centrifugation, and filtration). Finally, lyophilization was performed to produce powdered collagen that was used to prepare hydrogels used in the rest of this study. The total recoverable collagen yield from this fibroblast fixed-bed bioreactor culture system was 200 mg/L, corresponding to approximately 7.2 mg/L/day under the experimental conditions.

2.2. SDS-PAGE Analysis

SDS-PAGE was performed to evaluate the molecular characteristics of the CB collagen in comparison to a traditional AD bovine Type I collagen (Advanced Biomatrix, CA) (n = 1/group). Each sample was diluted to a protein concentration of 0.25 mg/mL and mixed with NuPAGE LDS sample buffer containing Coomassie G250 and Phenol Red. The mixtures were heated at 95 °C for 5 min to denature the proteins. Protein separation was carried out using a 3−8% gradient Tris-Acetate gel at a constant voltage of 150 V for approximately 60 min. A prestained protein ladder (Thermo Fisher Scientific, MA) was used as a molecular weight reference. After electrophoresis, the gels were stained with Coomassie Brilliant Blue for 20 min and subsequently destained with a solution containing 50% methanol and 10% acetic acid. Protein bands corresponding to collagen characteristic α-chains, β-dimers, and γ-trimers of collagen were analyzed to assess molecular composition. Band pattern and intensity were compared across the samples to evaluate the molecular weight distribution of the collagen.

2.3. Amino Acid Analysis

The amino acid composition of CB and AD bovine collagen was quantified to assess biochemical similarity. The samples were first hydrolyzed via overnight acid hydrolysis in 6 M HCl. Following hydrolysis, samples were neutralized with 6 M NaOH (1:1 v/v) and derivatized using the AccQ-Tag Ultra Derivatization Kit (Waters Corporation, MA), as per the manufacturer's instructions. Amino acid profiling was conducted using the ACQUITY UPLC H-Class system equipped with an AccQ-Tag Ultra column (1.7 μm, 2.1 × 100 mm^2). The separation was performed at 43 °C using a flow rate of 700 μL/min. The mobile phases consisted of 100% AccQ-Tag Ultra Eluent A and a 90:10 (v/v) mixture of water and Eluent B. A 1 μL injection volume was used for each sample and standard. Detection was carried out by UV absorbance at 260 nm. Quantification was performed using the Amino Acid Cell Culture Standard Kit (Waters Corporation, MA), which includes 26 amino acids. Standard curves were generated using serial dilutions from 500 pmol/μL to 1.5 pmol/μL. All chromatographic data were processed using Empower software (Waters Corporation, MA), and sample concentrations were calculated by comparing integrated peak areas to the standard curve.

2.4. Circular Dichroism Spectroscopy

Circular dichroism spectroscopy was used to examine the secondary structure of CB collagen and verify the presence of the triple-helical conformation. CB collagen samples were reconstituted in 0.25 M acetic acid at a final concentration of 0.12 mg/mL. The solution was transferred into a 1 mm path length quartz cuvette, and spectra were collected using a Chirascan V100 spectropolarimeter (Applied Photophysics, U.K.). Spectra were recorded from 190 to 260 nm at a scan speed of 20 nm/min with a data interval of 0.5 nm. Each measurement was performed at 10 °C. Characteristic spectral features indicating collagen's polyproline II helix were analyzed, consistent with literature-reported profiles of native type I collagen.[19]

2.5. DSC Analysis

The thermal stability of CB and AD collagen samples was evaluated using DSC. Approximately 5 mg of lyophilized collagen samples were sealed in aluminum Tzero pans (TA Instruments, DE), and an empty pan was used as a reference. The DSC analysis was conducted using a Discovery DSC 250 (TA Instruments, DE) over a temperature range of 30 °C to 250 °C with a heating rate of 20 °C/min under a nitrogen atmosphere. The thermogram was used to determine thermal denaturation properties, including the onset and peak denaturation

https://doi.org/10.1021/acsbiomaterials.5c02203
ACS Biomater. Sci. Eng. 2026, 12, 3177−3187

temperatures (T_{onset} and T_{peak}), which reflect the collagen's thermal stability.

2.6. Hydrogel Preparation

The same protocol was used to prepare hydrogels of both CB and AD collagen for rheological, mechanical, surface wettability, and biocompatibility testing. First, one part of chilled 10× PBS was gradually added to eight parts of chilled collagen, and the pH of the solution was carefully adjusted to 7.2−7.4 using sterile 0.1 M NaOH. Then, sterile DI water was added to bring the total volume to ten parts, resulting in a final collagen concentration of 8 mg/mL. Next, these solutions were cast into cylindrical molds (⌀8 × 4 mm^2) and incubated (37 °C, 5% CO_2) for 1 h to allow gelation.

2.7. Characterization of Rheological Properties

Rheological testing was performed at room temperature using an Anton Paar MCR 92 rheometer with a parallel plate geometry (Ø25 mm, 1 mm gap) to assess the CB and AD hydrogels' (n = 5/group) viscoelastic behavior and stability under deformation. Amplitude sweeps were performed at a constant frequency of 1 Hz over a strain range of 0.01−500% to determine the storage modulus (G′), loss modulus (G″), and loss tangent (tan δ = G″/G′), which provide insights into the hydrogels' ability to maintain their structure under applied forces. This rheological analysis focused on strain-dependent viscoelastic behavior at a fixed frequency (1 Hz) to establish the linear viscoelastic region (LVR) and compare relative modulus responses. The LVR, determined from the amplitude sweep, where the hydrogel's rheological properties remain constant under small deformations, was identified on the flow curves. Beyond the LVR, nonlinear deformation behavior was analyzed to understand the hydrogel's structural integrity under larger strains.

2.8. Characterization of Mechanical Properties

The compressive properties of the CB and AD collagen hydrogels were evaluated to assess their ability to withstand static and dynamic loading, which is especially important for load-bearing tissue engineering applications. Testing was performed using an Instron 5944 universal testing system following ASTM D638 protocols for hydrogel compression. The samples (⌀8 × 4 mm^2, n = 5/group) were subjected to unconfined compression testing, including static and dynamic loading. First, the hydrogels were compressed at a constant rate of 0.01 mm/s until reaching 20% strain, and the compressive modulus was determined as the slope of the linear region of the stress−strain curve. After completing the static compression, the sample was allowed to rest for 300 s to equilibrate and recover its structural integrity. Subsequently, cyclic compressive loads were applied within a strain range of 18−22% at the same displacement rate (0.01 mm/s), and dynamic modulus was determined from the stress−strain curves.

2.9. Characterization of Surface Wettability

The wettability of the CB and AD collagen hydrogels was evaluated via water contact angle (WCA) measurements at room temperature. Wettability impacts the material's behavior in aqueous biological environments and can directly influence cell adhesion, proliferation, and overall biocompatibility.[20] An 8 μL droplet of ultrapure water (Milli-Q, MA) was deposited onto the top surface of each sample (n = 3/group) and allowed to stabilize for a few seconds before high-resolution images were captured at a fixed angle to the surface. The contact angle formed between the water droplet and the hydrogel surface was analyzed using the Drop Shape Analysis plugin in ImageJ.[21]

2.10. Cell Viability and Proliferation Assessment

NIH/3T3 fibroblast cell viability and proliferation on CB and AD collagen hydrogels were evaluated to compare the biological performance of the two materials under identical culture conditions. The cells (1 × 10^6, ATCC, VA) were gently pipetted onto the surface of each CB and AD hydrogel, and the samples were cultured (37 °C, 5% CO_2) in complete media (DMEM supplemented with 10% FBS and 1% penicillin-streptomycin) for 7 days. Note that this cell seeding density is consistent with literature on NIH/3T3 fibroblast culture in three-dimensional hydrogel systems.[52,53] Cell viability was assessed (n = 3/group) on days 1, 3, and 7 using the Live/Dead assay (Thermo Fisher Scientific, MA). Herein, the samples were stained with calcein AM and ethidium homodimer-1 and fluorescence images were captured at each time point using a Leica DMi8 microscope. Quantitative analysis was performed using ImageJ to determine the cell density (cells/mm^2) and the total area covered by live cells (mm^2). Furthermore, cellular metabolic activity was assessed (n = 3/group) using the alamarBlue (aB) assay at days 1, 3, and 7. At each time point, the samples were cultured (37 °C, 5% CO_2) for 4 h in culture medium containing the aB reagent, and %aB reduction was calculated based on absorbance measurements using a microplate reader at 570 and 600 nm wavelengths.

2.11. Statistical Analysis

All experimental data were expressed as mean ± standard deviation. All comparisons (except biocompatibility assessment) between the CB and AD collagen hydrogels were analyzed using an unpaired t test (α = 0.05) in GraphPad Prism. The biocompatibility results were analyzed via two-way ANOVA and Tukey HSD post hoc tests (α = 0.05) in GraphPad Prism.

3. RESULTS AND DISCUSSION

3.1. Molecular Composition

The results of SDS-PAGE indicating the molecular composition of the CB collagen in comparison to the traditional AD collagen are presented in Figure 3. They highlight distinct

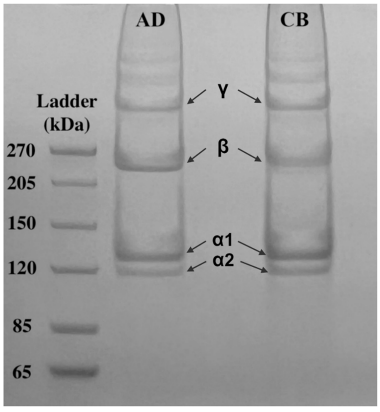


Figure 3. SDS-PAGE analysis showing molecular weight standards (reference ladder) on the left and characteristic bands for AD and CB collagen samples.

banding patterns in the CB collagen, which are consistent with the molecular structure of the AD control. Two clear and well-defined primary bands characteristic of type I collagen − α1-chains (~130 kDa) and α2-chains (~120 kDa) at expected 2:1 ratio, β-dimers (~240 kDa), and γ-trimers (~300 kDa)− were observed in both groups. These findings confirm the successful preservation of the CB collagen's native molecular composition during the cellular agriculture production process.

3.2. Amino Acid Composition

The amino acid profiles of CB and AD bovine collagens are shown in Table 1. Both collagen types demonstrated nearly identical amino acid compositions, with glycine, proline, and hydroxyproline being the most abundant residues, which are characteristic of type I collagen. Glycine accounted for approximately one-third of the total residues in both samples, consistent with the Gly-X-Y repeating motif found in the collagen triple helix. Minor variations (within ± 3%) were observed across all residues except proline; however, no

https://doi.org/10.1021/acsbiomaterials.5c02203
ACS Biomater. Sci. Eng. 2026, 12, 3177−3187

Table 1. Amino Acid Composition of CB and AD Bovine Collagen

Sample concentrations (per 1000 amino acids)					
Amino acid	CB collagen	AD collagen	Amino acid	CB collagen	AD collagen
HyPro	103.07	101.58	HyLys1	<	1.55
His	<	<	HyLys2	18.40	17.11
Asn	<	<	AABA	<	<
Tau	<	<	Orn	N/A	N/A
Ser	38.73	37.93	Cys	22.42	23.42
Gln	27.08	26.55	Lys	22.83	23.26
Arg	<	<	Tyr	<	<
Gly	338.29	332.57	Met	<	<
Asp	48.5	48.35	Val	16.16	15.86
Glu	75.64	74.89	Ile	<	<
Thr	19.33	19.03	Trp	25.62	23.48
Ala	124.80	122.36	Leu	<	<
GABA	<	<	Phe	<	<
Pro	119.14	132.06	total	1000.00	1000.00

statistically significant differences were detected for any amino acid. These findings confirm that the amino acid profile of CB collagen closely mirrors that of native AD collagen.

3.3. Secondary Structure

The circular dichroism spectrum of CB collagen is presented in Figure 4. It exhibited spectral signatures consistent with the

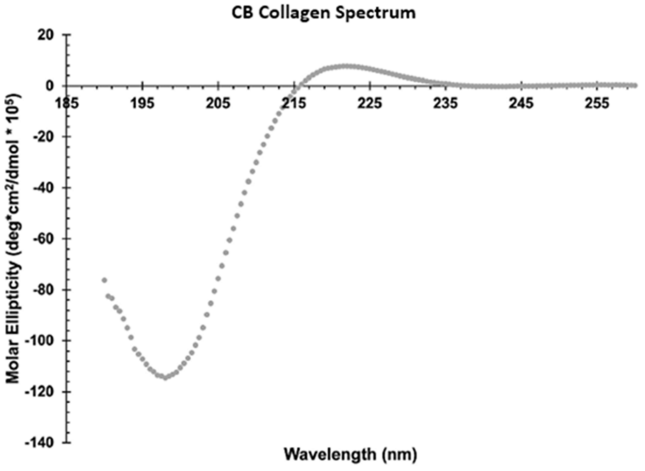


Figure 4. Circular dichroism spectrum of CB bovine collagen showing the characteristic polyproline II helical signature (large negative value in the 195−205 nm range and smaller positive value near 220 nm).

polyproline II (PPII) helical conformation typical of native collagen.[19] Specifically, the resulting curve shows the characteristic polyproline II helical signature (large negative value in the 195−205 nm range, smaller positive value near 220 nm), indicating the molecule is in its native triple helical form with secondary structure intact. These results indicate that CB collagen retains the native secondary structure of type I collagen, with proper folding and triple-helix formation.

3.4. Thermal Properties

Thermal profiles of CB and AD collagen, assessed by DSC, are shown in Figure 5. Both samples exhibited nearly identical thermograms, with the onset temperature (T_{onset}) occurring at approximately 150−151 °C and the peak transition temperature (T_{peak}) at approximately 151−153 °C. The prominent

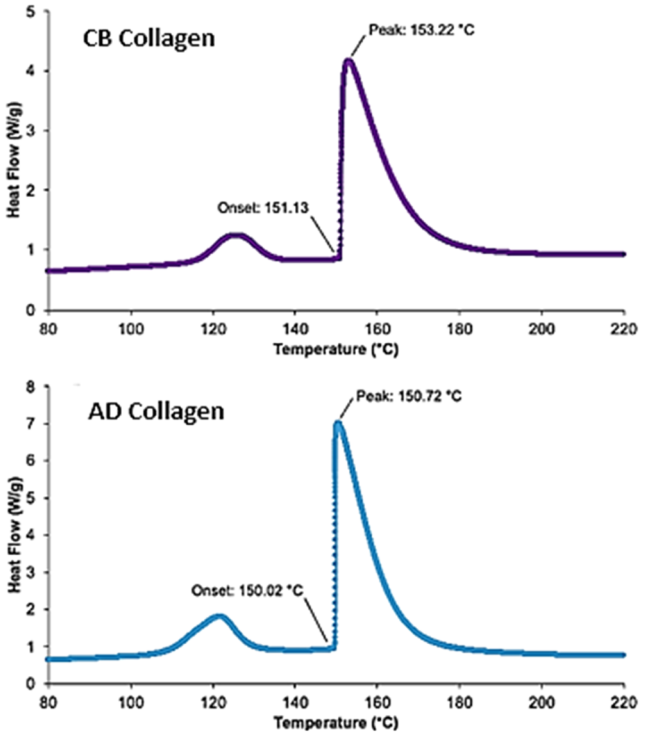


Figure 5. DSC thermograms of lyophilized CB and AD collagen samples showing nearly identical onset and peak heat flow profiles.

endothermic transition observed near 150 °C for both CB and AD collagen is interpreted as a major thermal transition that reflects overlapping helix destabilization and thermally induced degradation processes under the experimental conditions employed.[22] The relatively sharp peak shape and near-vertical onset temperature (T_{onset}) observed for this transition may also be influenced by kinetic and instrumental factors associated with DSC measurements of lyophilized samples. In particular, the relatively high heating rate (20 °C min^{-1}) accentuates the apparent abruptness of the transition due to thermal lag between the sample and the sensor, while sealed pan conditions promote transient pressure build-up arising from the release of bound moisture or volatile degradation products.[23] The smaller endothermic feature between 110−120 °C is attributed to the loss of residual or bound water associated with the lyophilized collagen matrix, a phenomenon commonly observed in dried biopolymer systems.[24] The similarity in thermal transition behavior indicates that the CB collagen produced via cellular agriculture retains thermal stability equivalent to that of AD collagen.

3.5. Rheological Properties

Representative rheograms and comparisons of the storage modulus (G′) representing the elastic response and the loss modulus (G″) representing the viscous response (i.e., energy dissipation) of the CB and AD hydrogels are presented in Figure 6a−d.

Although in the same order of magnitude, the G′ and G″ of the CB collagen (48.40 ± 8.5 Pa and 13.20 ± 1.3 Pa, respectively) were significantly higher ($p < 0.05$ and $p < 0.01$, respectively) than those of the AD controls (25 ± 2.12 Pa and 10 ± 1.58 Pa, respectively). Furthermore, the loss tangent (tan δ) of the CB collagen (0.27 ± 0.02) was significantly lower ($p < 0.01$) than that of the AD collagen (0.39 ± 0.03), denoting its higher elasticity and reduced energy dissipation. These

https://doi.org/10.1021/acsbiomaterials.5c02203
ACS Biomater. Sci. Eng. 2026, 12, 3177−3187

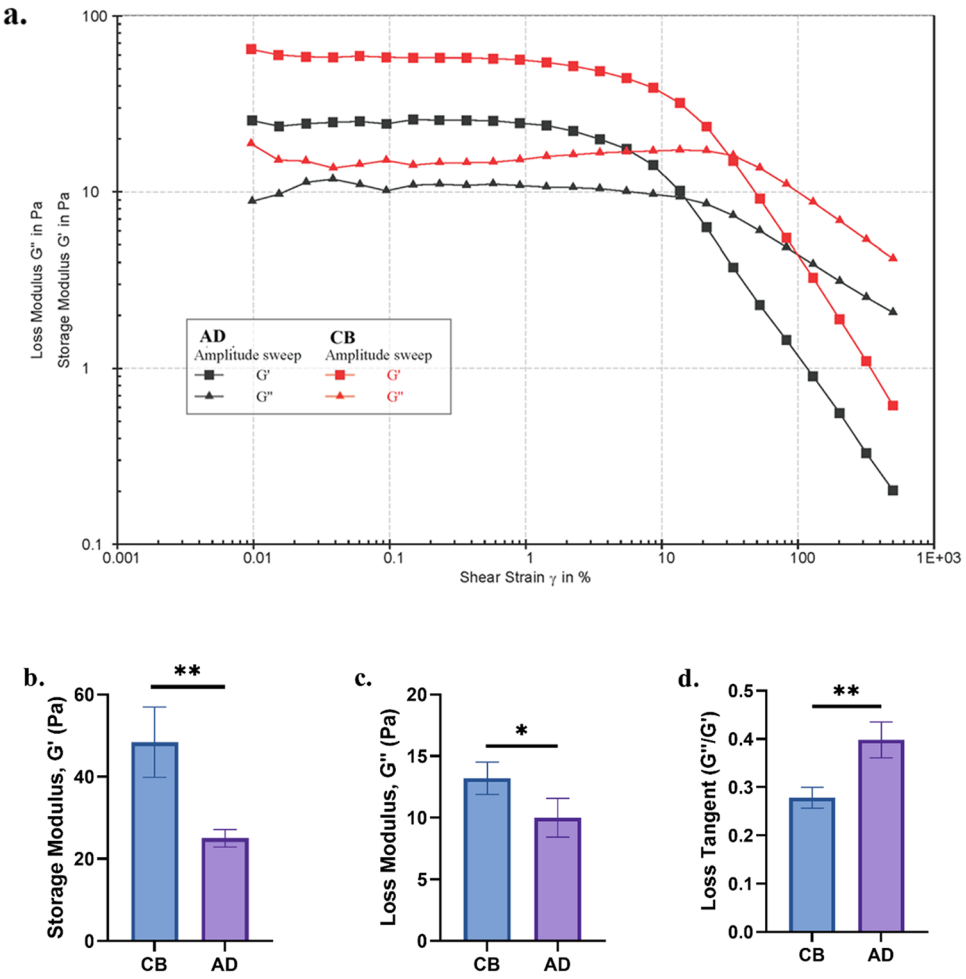


Figure 6. (a) Flow curves (rheograms) for CB and AD collagen hydrogels; (b–d) Comparative analysis of storage modulus, loss modulus, and loss tangent, respectively, between CB and AD collagen hydrogels, with significance indicated as $*p \leq 0.05$ and $**p \leq 0.01$.

findings demonstrate that CB collagen hydrogels possessed higher structural stability and elasticity, which are potentially suitable for biofabrication processes such as extrusion-based bioprinting.[25] The balance between elasticity (G′) and viscosity (G″) ensures that the hydrogels can maintain their structure during and after biofabrication, an essential property for creating scaffolds for biomedical and cultivated meat applications.[26] In extrusion-based bioprinting, this strain-dependent viscoelastic behavior is critical as it enables the hydrogel to flow smoothly under shear stress during extrusion while recovering its shape upon deposition. Higher elasticity (G′) ensures the printed filaments retain their geometry and do not collapse, while an optimal viscous response (G″) ensures smooth extrusion without clogging or inconsistencies.[27,28]

3.6. Mechanical Properties

Representative stress–strain curves from the two-stage unconfined compression testing and the corresponding moduli of the CB and AD hydrogels are presented in Figure 7a–c. Both the compressive and the dynamic moduli of the CB hydrogels (1260 ± 191 Pa and 6250 ± 1031 Pa, respectively) were significantly higher ($p < 0.05$) than those of the AD controls (890 ± 255 Pa and 3134 ± 1857 Pa, respectively), indicating higher stiffness and resistance to deformation under both static and cyclic loading. These results highlight CB collagen hydrogel's ability to maintain structural integrity in dynamic biological environments. As such, these compressive and dynamic moduli are in the same range as hydrogel scaffolds used in skin and muscle tissue engineering.[29−31] While lower stiffness in scaffolding materials has been shown to aid in better maintenance of cell *stemness*, higher stiffness is beneficial for cell differentiation.[32] These values may overlap and ultimately depend on the cell type and application.

3.7. Surface Wettability

Representative images comparing the surface wettability of the CB and AD collagen hydrogels are presented in Figure 8. Both hydrogels were found to be hydrophilic (WCA < 90°), although the WCA of the CB collagen (35 ± 2°) was lower than that of the AD control (40 ± 3°). The relatively lower contact angle indicates a higher degree of hydrophilicity, which may be beneficial for promoting cell adhesion and proliferation. This hydrophilic property is essential for scaffolds used in biomedical applications, promoting compatibility and interaction with biological tissues.[33,34] The hydrophilicity of gels is also important for food applications as it enhances water retention, improves texture and mouthfeel, and facilitates the delivery of water-soluble nutrients and flavors, making it ideal for mimicking the moisture and tenderness of natural food components.[35]

https://doi.org/10.1021/acsbiomaterials.5c02203
ACS Biomater. Sci. Eng. 2026, 12, 3177−3187

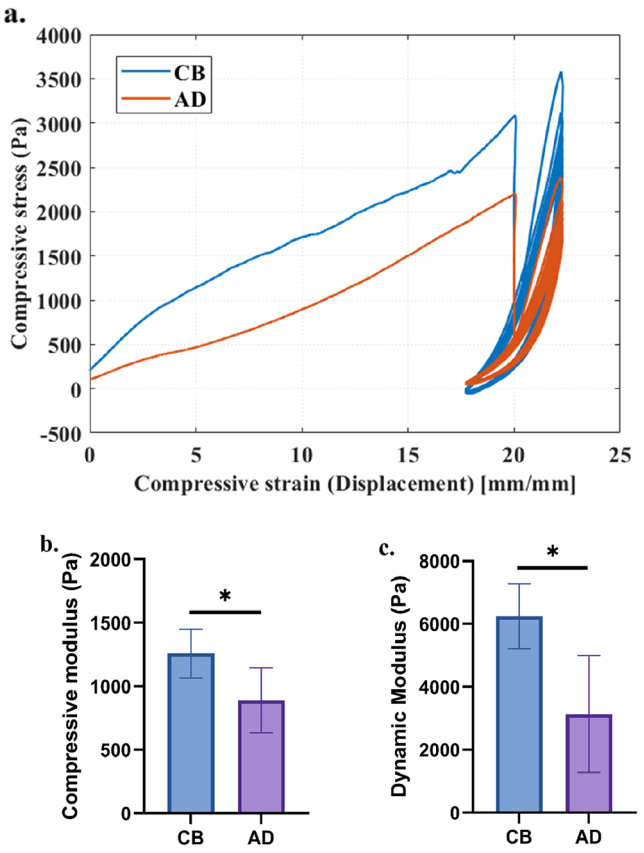


Figure 7. (a) Representative stress−strain curves from unconfined compression testing; (b, c) Comparison of compressive modulus and dynamic modulus, respectively, between CB and AD collagen hydrogels, with significance indicated as $*p \leq 0.05$.

3.8. Cell Viability and Proliferation

Results of cell viability assessment are summarized in Figure 9a−d and show >96% viability across all time points in both hydrogels. The cell density in CB collagen hydrogels increased from day 1 (329 ± 34 cells/mm^2) to day 3 (772 ± 25 cells/mm^2) and day 7 (907 ± 14 cells/mm^2). This trend was similar to that observed in AD collagen hydrogels wherein the cell density increased from day 1 (390 ± 58 cells/mm^2) to day 3 (838 ± 47 cells/mm^2) and day 7 (1087 ± 25 cells/mm^2). Similarly, the area covered by live cells in CB collagen hydrogels increased from day 1 (1.21 ± 0.26 mm^2) to day 3 (2.84 ± 0.48 mm^2) and day 7 (3.04 ± 0.39 mm^2), with a similar trend observed in AD collagen hydrogels (an increase from 1.49 ± 0.21 mm^2 to 3.02 ± 0.35 mm^2 and 3.90 ± 0.58 mm^2 on days 1, 3 and 7, respectively). Metabolic activity indicated by %aB reduction supported these findings, in that the %aB reduction in CB collagen hydrogels increased from 31.97 ± 0.92 on day 1 to 40.10 ± 0.85 on day 3 and 53.73 ± 1.91 on day 7, compared to 34.39 ± 1.18 on day 1, 52.97 ± 0.85 on day 3, and 65.98 ± 0.69 on day 7 for AD collagen hydrogels. Results of two-way ANOVA showed statistically significant differences in cell density, live cell area coverage, and metabolic activity between CB and AD sample groups at different time points ($p < 0.05$). Post hoc analysis revealed that while there were no significant differences in cell density, live cell area, or metabolic activity on day 1, by day 7, there were statistically significant differences ($p < 0.05$) between CB and AD collagen hydrogels across all three metrics. These results, summarized in Figure 9b−d, demonstrate that the CB collagen hydrogel demonstrated good biocompatibility and cell proliferation, although it was, statistically speaking, lower than that observed in AD collagen.

3.9. Discussion

The results of this study demonstrate the general similarities between important molecular, structural, mechanical, and biological characteristics of CB collagen produced via cellular agriculture in comparison to its traditional AD counterpart. The preservation of collagen's molecular composition in the CB collagen, as indicated by the characteristic α-chains (~120 kDa) and β-dimers (~240 kDa) in SDS-PAGE analysis, is crucial for maintaining its bioactivity and functionality in biological applications.[36,37]

Amino acid analysis confirmed the biochemical equivalence between CB and AD collagen, with both materials exhibiting nearly identical amino acid compositions dominated by glycine, proline, and hydroxyproline, the hallmark residues responsible for triple-helix stabilization and tensile strength in type I collagen.[11] These results underscore the effectiveness of mammalian cell platforms in replicating the key biosynthetic steps of collagen, including hydroxylation of proline and lysine. Notably, hydroxyproline levels, a critical marker of post-translational modification and triple-helix stability,[37] were equivalent between CB and AD collagen. These findings confirm that the amino acid profile of CB collagen closely mirrors that of native collagen, supporting its structural and functional equivalence.

Circular dichroism spectroscopy revealed a strong negative ellipticity near 197 nm and a positive peak around 220 nm in CB collagen, consistent with the polyproline II helical conformation of native triple-helical collagen.[19] This secondary structure is essential for collagen's biological recognition by integrins and its mechanical resilience.[38] In addition, DSC showed comparable onset and peak denaturation temperatures (~150 °C) for both CB and AD collagen, confirming equivalent thermal stability. These results suggest that CB collagen maintains native-like molecular packing and intramolecular hydrogen bonding, features critical for preserving structural integrity during physiological function and bioprocessing.[11,39] This is particularly important for biomaterials such as collagen that may undergo thermal sterilization processes, such as autoclaving, and must retain their functional properties post-treatment.[40]

The CB collagen hydrogels exhibited significantly higher G′ (48.40 ± 8.5 Pa) and G″ (13.20 ± 1.3 Pa) but lower loss tangent (0.27 ± 0.02) than AD collagen, indicating higher elasticity and reduced energy dissipation. These properties

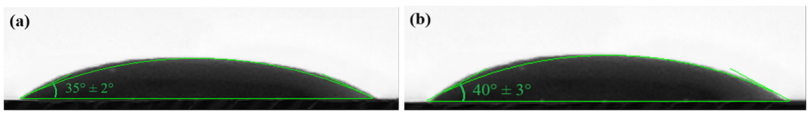


Figure 8. Water Contact Angle measurement for (a) CB and (b) AD collagen hydrogels.

https://doi.org/10.1021/acsbiomaterials.5c02203
ACS Biomater. Sci. Eng. 2026, 12, 3177−3187

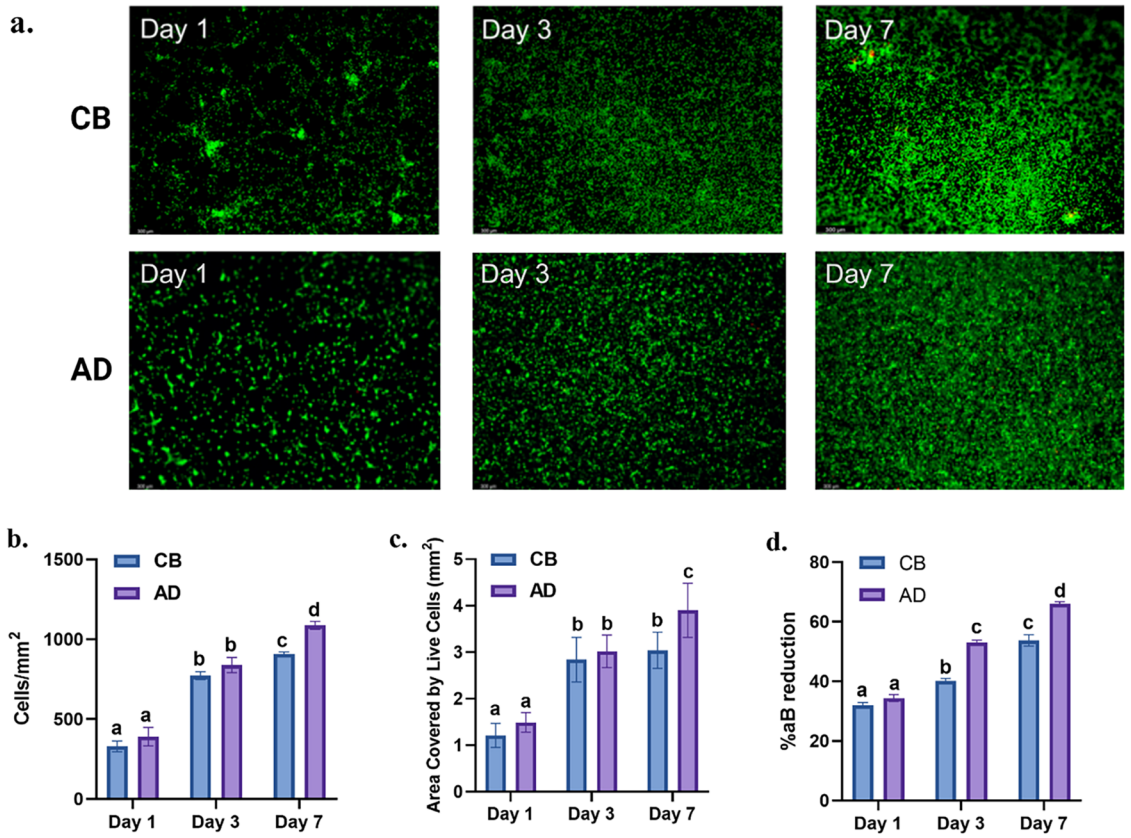


Figure 9. Results from biocompatibility assessment of the CB and AD collagen hydrogels at days 1, 3, and 7 in culture: (a) representative Live/Dead images; (b, c) ImageJ quantitative analysis results for number of cells per mm^2, and area covered by the live cells in mm^2, respectively; and (d) %aB reduction corresponding to cellular metabolic activity. (Data points which do not share a common letter are significantly different, with significance $p \leq 0.05$).

suggest that CB collagen hydrogels can maintain their structure under mechanical stress, making them well-suited for biofabrication via processes such as extrusion three-dimensional (3D) bioprinting. The combination of higher elasticity and mechanical resilience indicates that CB collagen may be able to withstand shear forces during printing while retaining its shape postdeposition, which is essential for fabricating complex tissue scaffolds.[41,42] Additionally, CB collagen's observed viscoelastic behavior would ensure smooth extrusion under shear stress and rapid recovery of shape upon deposition in extrusion-based 3D bioprinting.[43]

The mechanical properties of CB collagen hydrogel highlight its potential for a wide range of biomedical applications. The compressive modulus (1260 ± 191 Pa) and dynamic modulus (6250 ± 1031 Pa) were significantly higher than those of AD collagen, indicating greater stiffness and resistance to deformation under cyclic loading. This suggests that the CB collagen hydrogel may be particularly advantageous for applications requiring mechanical durability, where maintaining structural integrity under biomechanical loading is critical. These properties align well with soft tissue engineering applications, particularly for soft tissue and cartilage repair, which require moduli within the 600−3000 Pa range.[44−46]

Furthermore, tissue engineering scaffolds must strike a balance between mechanical support and flexibility to facilitate cell growth and tissue remodeling.[47] Past research indicated that scaffold stiffness plays a crucial role in directing cell behavior, with increased stiffness enhancing mesenchymal stem cell differentiation due to substrate mechanosensitivity.[48] Based on our mechanical and rheological characterization, the CB collagen hydrogel exhibits properties suitable for modulating cell fate, highlighting its potential for use in targeted regenerative therapies.

The CB collagen hydrogel also demonstrated increased hydrophilicity (contact angle = 35 ± 2°). This is advantageous for biomedical applications as it enhances protein adsorption and integrin-mediated cell adhesion, leading to improved cell proliferation.[49,50] Additionally, in cultivated meat applications, hydrophilic scaffolds can aid in moisture retention to improve texture and mouthfeel.[51]

CB collagen hydrogel supported fibroblast viability, proliferation, and metabolic activity over 7 days in culture, although it was outperformed by the AD collagen. Nonetheless, the significant increase in cell density (329 ± 34 to 907 ± 14 cells/mm^2) and metabolic activity (31.97% to 53.73% aB reduction) highlights CB collagen's potential for biomedical applications, such as wound healing scaffolds, bioartificial skin, and ECM-based implants.[54−57] While traditional collagen sources often suffer from batch-to-batch variability due to inherent interanimal biological differences, immunogenicity concerns, and pathogen risks,[58,59] CB collagen can provide a standardized, reproducible, and ethical alternative.

Results from molecular, biochemical, structural, thermal, rheological, mechanical, and biological assessments collectively indicate that CB collagen produced via cellular agriculture exhibits broad equivalence to traditional AD collagen, with some properties showing favorable trends. These findings establish a performance baseline for collagen produced via

https://doi.org/10.1021/acsbiomaterials.5c02203
ACS Biomater. Sci. Eng. 2026, 12, 3177−3187

cellular agriculture and highlights its potential as an animal-free alternative for biomedical and food applications. At the same time, they also highlight important opportunities for continued research needed to advance cellular agriculture technology. As fibroblast proliferation and metabolic activity on CB collagen were acceptable yet statistically lower than AD collagen, future research should prioritize improving the inherent biocompatibility of CB collagen through refinements in upstream cellular agriculture processes. These may include optimizing the cell culture conditions to enhance essential post-translational modifications (e.g., proline and lysine hydroxylation) as well as controlling fibrillogenesis during production to more closely replicate the hierarchical architecture of native collagen. In parallel, research should also focus on optimizing bioprocessing conditions to improve yield, purity, and biomechanical performance, as well as conducting long-term stability studies to establish performance under physiological and industrial processing conditions. Investigating strategies such as genetic modifications or alternative cell sources could enable CB collagen with composition and biofunctional profiles tailored for application-specific requirements, including implants, tissue scaffolds, and cultivated meat structures.[40,58,60] To advance translational use, studies should evaluate CB collagen in relevant tissue engineering contexts using appropriate cell types and scaffold geometries, and systematically assess bioprintability parameters such as print fidelity, structural retention, and postprinting stability. Finally, assessing cost-effectiveness and scalability will be critical for enabling adoption across biomedical and food industries in the long term.

While this study does not present a full industrial scale-up analysis, the volumetric yield (~200 mg/L total; ~7.2 mg/L/day) achieved using fibroblast culture in our lab-scale fixed-bed bioreactor system exceeds reported yields (~0.5 mg/L)[61] for full-length Type I collagen in mammalian recombinant platforms. These findings suggest that cellular agriculture-based collagen production may offer meaningful productivity advantages while maintaining native structural fidelity; however, detailed techno-economic and scale-up analyses remain necessary.

4. CONCLUSION

This study demonstrates that Type I bovine collagen produced via cellular agriculture can closely match the structural and functional properties of traditional animal-derived collagen, providing a controlled, animal-free production alternative for biomedical, food, and cosmetic applications. The CB collagen retained biochemical and structural features characteristic of AD collagen, exhibited favorable rheological and mechanical properties, and supported good fibroblast viability and proliferation, although the cellular activity was lower than AD collagen. Collectively, these results establish a clear performance baseline for collagen produced via cellular agriculture and highlight opportunities for continued development. Future work should prioritize enhancing the material's inherent biocompatibility as well as yield and purity through upstream process optimization. Additional efforts should focus on systematic evaluation of bioprintability, scaffold design, long-term stability, and manufacturing scalability to advance reliable, application-specific translation of CB collagen across industry sectors.

AUTHOR INFORMATION

Corresponding Author

Rohan A. Shirwaiker − *Edward P. Fitts Department of Industrial and Systems Engineering, North Carolina State University, Raleigh, North Carolina 27695, United States; Bezos Center for Sustainable Protein at North Carolina State University, Raleigh, North Carolina 27695, United States; Departments of Mechanical and Aerospace Engineering and Biomedical Engineering, North Carolina State University, Raleigh, North Carolina 27695, United States;* orcid.org/0000-0002-0215-2847; Email: rashirwa@ncsu.edu

Authors

Nafi Ahmed − *Edward P. Fitts Department of Industrial and Systems Engineering, North Carolina State University, Raleigh, North Carolina 27695, United States; Bezos Center for Sustainable Protein at North Carolina State University, Raleigh, North Carolina 27695, United States*

Corbin M. Goodwin − *Edward P. Fitts Department of Industrial and Systems Engineering, North Carolina State University, Raleigh, North Carolina 27695, United States; Bezos Center for Sustainable Protein at North Carolina State University, Raleigh, North Carolina 27695, United States*

Megan Hales − *Jellatech Inc., Morrisville, North Carolina 27560, United States*

Juan Camacho − *Jellatech Inc., Morrisville, North Carolina 27560, United States*

Christopher Gilchrist − *Jellatech Inc., Morrisville, North Carolina 27560, United States*

Complete contact information is available at: https://pubs.acs.org/10.1021/acsbiomaterials.5c02203

Author Contributions

N.A., C.G., and R.A.S. conceptualized the study. N.A., C.M.G., M.H., J.C., C.G., and R.A.S. contributed to methodology, investigation, data analysis, and preparation of the original draft. N.A., C.G., and R.A.S. contributed to writing−review and editing. C.G. and R.A.S. supervised the research. R.A.S. managed project administration and funding acquisition. R.A.S. and C.G. provided resources.

Notes

The authors declare the following competing financial interest(s): M.H., J.C., and C.G. are employees of Jellatech Inc., which produced the CB collagen using their proprietary cell culture technology.

ACKNOWLEDGMENTS

Jellatech Inc. provided some of the experimental materials used in this study. This work was supported, in part, by the Bezos Center for Sustainable Protein at NC State through a grant from the Bezos Earth Fund.

REFERENCES

(1) Henchion, M.; Hayes, M.; Mullen, A. M.; Fenelon, M.; Tiwari, B. Future Protein Supply and Demand: Strategies and Factors Influencing a Sustainable Equilibrium. *Foods* **2017**, *6* (7), No. 53.

(2) Kumagai, S.; Daikai, T.; Onodera, T. Bovine Spongiform Encephalopathy − A Review from the Perspective of Food Safety. *Food Saf.* **2019**, *7* (2), 21−47.

(3) Van Eenennaam, A. L.; Werth, S. J. Animal Board Invited Review: Animal Agriculture and Alternative Meats − Learning from

Past Science Communication Failures. *Animal* **2021**, *15* (10), No. 100360.
(4) Yue, C.; Ding, C.; Xu, M.; Hu, M.; Zhang, R. Self-Assembly Behavior of Collagen and Its Composite Materials: Preparation, Characterizations, and Biomedical Engineering and Allied Applications. *Gels* **2024**, *10* (10), No. 642.
(5) Irastorza, A.; Zarandona, I.; Andonegi, M.; Guerrero, P.; de la Caba, K. The Versatility of Collagen and Chitosan: From Food to Biomedical Applications. *Food Hydrocolloids* **2021**, *116*, No. 106633.
(6) Xu, N.; Peng, X.-L.; Li, H.-R.; Liu, J.-X.; Cheng, J.-S.-Y.; Qi, X.-Y.; Ye, S.-J.; Gong, H.-L.; Zhao, X.-H.; Yu, J.; Xu, G.; Wei, D.-X. Marine-Derived Collagen as Biomaterials for Human Health. *Front. Nutr.* **2021**, *8*, No. 702108, DOI: 10.3389/fnut.2021.702108.
(7) Espinales, C.; Romero-Peña, M.; Calderón, G.; Vergara, K.; Cáceres, P. J.; Castillo, P. Collagen, Protein Hydrolysates and Chitin from by-Products of Fish and Shellfish: An Overview. *Heliyon* **2023**, *9* (4), No. e14937.
(8) Fasciano, S.; Wheba, A.; Ddamulira, C.; Wang, S. Recent Advances in Scaffolding Biomaterials for Cultivated Meat. *Biomater. Adv.* **2024**, *162*, No. 213897.
(9) Soleymani, S.; Naghib, S. M.; Mozafari, M. R. An Overview of Cultured Meat and Stem Cell Bioprinting: How to Make It, Challenges and Prospects, Environmental Effects, Society's Culture and the Influence of Religions. *J. Agric. Food Res.* **2024**, *18*, No. 101307.
(10) Bomkamp, C.; Skaalure, S. C.; Fernando, G. F.; Ben-Arye, T.; Swartz, E. W.; Specht, E. A. Scaffolding Biomaterials for 3D Cultivated Meat: Prospects and Challenges. *Adv. Sci.* **2022**, *9* (3), No. 2102908.
(11) Shoulders, M. D.; Raines, R. T. Collagen Structure and Stability. *Annu. Rev. Biochem.* **2009**, *78*, 929−958.
(12) Xu, Y.; Keene, D. R.; Bujnicki, J. M.; Höök, M.; Lukomski, S. Streptococcal Scl1 and Scl2 Proteins Form Collagen-like Triple Helices. *J. Biol. Chem.* **2002**, *277* (30), 27312−27318.
(13) Fertala, A. Three Decades of Research on Recombinant Collagens: Reinventing the Wheel or Developing New Biomedical Products? *Bioengineering* **2020**, *7* (4), No. 155.
(14) Amirrah, I. N.; Lokanathan, Y.; Zulkiflee, I.; Wee, M. F. M. R.; Motta, A.; Fauzi, M. B. A Comprehensive Review on Collagen Type I Development of Biomaterials for Tissue Engineering: From Biosynthesis to Bioscaffold. *Biomedicines* **2022**, *10* (9), No. 2307.
(15) Narayanan, A. S.; Page, R. C.; Swanson, J. Collagen Synthesis by Human Fibroblasts. Regulation by Transforming Growth Factor-Beta in the Presence of Other Inflammatory Mediators. *Biochem. J.* **1989**, *260* (2), 463−469.
(16) Tajima, S.; Pinnell, S. R. Collagen Synthesis by Human Skin Fibroblasts in Culture: Studies of Fibroblasts Explanted from Papillary and Reticular Dermis. *J. Invest. Dermatol.* **1981**, *77* (5), 410−412.
(17) Jalkanen, M.; Penttinen, R. Enhanced Fibroblast Collagen Production by a Macrophage-Derived Factor (CEMF). *Biochem. Biophys. Res. Commun.* **1982**, *108* (2), 447−453.
(18) McNulty, M. J.; Stout, A. J.; Kaplan, D. L. Meating the Moment. *EMBO Rep.* **2025**, *26* (13), 3229−3235.
(19) Ghosh, M.; Bera, S.; Schiffmann, S.; Shimon, L. J. W.; Adler-Abramovich, L. Collagen-Inspired Helical Peptide Coassembly Forms a Rigid Hydrogel with Twisted Polyproline II Architecture. *ACS Nano* **2020**, *14* (8), 9990−10000.
(20) How Surface Roughness and Wettability Affects Biocompatibility. https://www.biolinscientific.com/blog/how-surface-roughness-and-wettability-affects-biocompatibility-0 (accessed March 25, 2025).
(21) BIG > Drop Analysis. https://bigwww.epfl.ch/demo/dropanalysis/ (accessed March 23, 2025).
(22) Bozec, L.; Odlyha, M. Thermal Denaturation Studies of Collagen by Microthermal Analysis and Atomic Force Microscopy. *Biophys. J.* **2011**, *101* (1), 228−236.
(23) Gao, M.; Zhao, S.; Yang, H.; Wu, X.; Xiao, Y. An Analysis of the Influence of DSC Parameters on the Measurement of the Thermal Properties of Phase-Change Material. *Materials* **2024**, *17* (23), No. 5689.
(24) Samouillan, V.; Delaunay, F.; Dandurand, J.; Merbahi, N.; Gardou, J.-P.; Yousfi, M.; Gandaglia, A.; Spina, M.; Lacabanne, C. The Use of Thermal Techniques for the Characterization and Selection of Natural Biomaterials. *J. Funct. Biomater.* **2011**, *2* (3), 230−248.
(25) Naghieh, S.; Chen, X. Printability−A Key Issue in Extrusion-Based Bioprinting. *J. Pharm. Anal.* **2021**, *11* (5), 564−579.
(26) Hull, S. M.; Brunel, L. G.; Heilshorn, S. C. 3D Bioprinting of Cell-Laden Hydrogels for Improved Biological Functionality. *Adv. Mater.* **2022**, *34* (2), No. e2103691.
(27) de Miranda, L. R. M.; Jovanović, B.; Lesage, K.; De Schutter, G. Geometric Conformability of 3D Concrete Printing Mixtures from a Rheological Perspective. *Materials* **2023**, *16* (21), No. 6864.
(28) Herrada-Manchón, H.; Fernández, M. A.; Aguilar, E. Essential Guide to Hydrogel Rheology in Extrusion 3D Printing: How to Measure It and Why It Matters? *Gels* **2023**, *9* (7), No. 517.
(29) O'Bryan, C. S.; Ni, Y.; Taylor, C. R.; Angelini, T. E.; Schulze, K. D. Collagen Networks under Indentation and Compression Behave Like Cellular Solids. *Langmuir* **2024**, *40* (8), 4228−4235.
(30) Anderson, D. E.; Johnstone, B. Dynamic Mechanical Compression of Chondrocytes for Tissue Engineering: A Critical Review. *Front. Bioeng. Biotechnol.* **2017**, *5*, No. 76, DOI: 10.3389/fbioe.2017.00076.
(31) Zhang, Y.; Wang, Y.; Li, Y.; Yang, Y.; Jin, M.; Lin, X.; Zhuang, Z.; Guo, K.; Zhang, T.; Tan, W. Application of Collagen-Based Hydrogel in Skin Wound Healing. *Gels* **2023**, *9* (3), No. 185.
(32) Bodiou, V.; Moutsatsou, P.; Post, M. J. Microcarriers for Upscaling Cultured Meat Production. *Front. Nutr.* **2020**, *7*, No. 10, DOI: 10.3389/fnut.2020.00010.
(33) Webb, K.; Hlady, V.; Tresco, P. A. Relative Importance of Surface Wettability and Charged Functional Groups on NIH 3T3 Fibroblast Attachment, Spreading, and Cytoskeletal Organization. *J. Biomed. Mater. Res.* **1998**, *41* (3), 422−430.
(34) Menzies, K. L.; Jones, L. The Impact of Contact Angle on the Biocompatibility of Biomaterials. *Optom. Vis. Sci.* **2010**, *87* (6), 387−399.
(35) Nath, P. C.; Debnath, S.; Sridhar, K.; Inbaraj, B. S.; Nayak, P. K.; Sharma, M. A Comprehensive Review of Food Hydrogels: Principles, Formation Mechanisms, Microstructure, and Its Applications. *Gels* **2023**, *9* (1), No. 1.
(36) Fatiroi, N. S.; Jaziri, A. A.; Shapawi, R.; Mokhtar, R. A. M.; Noordin, W. N. M.; Huda, N. Biochemical and Microstructural Characteristics of Collagen Biopolymer from Unicornfish (Naso Reticulatus Randall, 2001) Bone Prepared with Various Acid Types. *Polymers* **2023**, *15* (4), No. 1054.
(37) Fidler, A. L.; Boudko, S. P.; Rokas, A.; Hudson, B. G. The Triple Helix of Collagens − an Ancient Protein Structure That Enabled Animal Multicellularity and Tissue Evolution. *J. Cell Sci.* **2018**, *131* (7), No. jcs203950.
(38) Miles, C. A.; Bailey, A. J. Thermally Labile Domains in the Collagen Molecule. *Micron* **2001**, *32* (3), 325−332.
(39) Miles, C. A.; Knott, L.; Sumner, I. G.; Bailey, A. J. Differences between the Thermal Stabilities of the Three Triple-Helical Domains of Type IX Collagen. *J. Mol. Biol.* **1998**, *277* (1), 135−144.
(40) Meyer, M. Processing of Collagen Based Biomaterials and the Resulting Materials Properties. *BioMed. Eng. OnLine* **2019**, *18* (1), No. 24.
(41) Debnath, S.; Agrawal, A.; Jain, N.; Chatterjee, K.; J Player, D. Collagen as a Bio-Ink for 3D Printing: A Critical Review. *J. Mater. Chem. B* **2025**, *13* (6), 1890−1919.
(42) Schwab, A.; Levato, R.; D'Este, M.; Piluso, S.; Eglin, D.; Malda, J. Printability and Shape Fidelity of Bioinks in 3D Bioprinting. *Chem. Rev.* **2020**, *120* (19), 10850−10877.
(43) Karvinen, J.; Kellomäki, M. Design Aspects and Characterization of Hydrogel-Based Bioinks for Extrusion-Based Bioprinting. *Bioprinting* **2023**, *32*, No. e00274.

(44) Liu, J.; Zheng, H.; Poh, P. S. P.; Machens, H.-G.; Schilling, A. F. Hydrogels for Engineering of Perfusable Vascular Networks. *Int. J. Mol. Sci.* **2015**, *16* (7), 15997−16016.
(45) Hafezi, M.; Khorasani, S. N.; Zare, M.; Neisiany, R. E.; Davoodi, P. Advanced Hydrogels for Cartilage Tissue Engineering: Recent Progress and Future Directions. *Polymers* **2021**, *13* (23), No. 4199.
(46) Wang, W.; Shi, Y.; Lin, G.; Tang, B.; Li, X.; Zhang, J.; Ding, X.; Zhou, G. Advances in Mechanical Properties of Hydrogels for Cartilage Tissue Defect Repair. *Macromol. Biosci.* **2023**, *23* (7), No. 2200539.
(47) Chan, B. P.; Leong, K. W. Scaffolding in Tissue Engineering: General Approaches and Tissue-Specific Considerations. *Eur. Spine J.* **2008**, *17* (Suppl 4), 467−479.
(48) Yi, B.; Xu, Q.; Liu, W. An Overview of Substrate Stiffness Guided Cellular Response and Its Applications in Tissue Regeneration. *Bioact. Mater.* **2022**, *15*, 82−102.
(49) Krishna, O. D.; Jha, A. K.; Jia, X.; Kiick, K. L. Integrin-Mediated Adhesion and Proliferation of Human MCs Elicited by A Hydroxyproline-Lacking, Collagen-like Peptide. *Biomaterials* **2011**, *32* (27), 6412−6424.
(50) Kim, H. S.; Kumbar, S. G.; Nukavarapu, S. P. Biomaterial-Directed Cell Behavior for Tissue Engineering. *Curr. Opin. Biomed. Eng.* **2021**, *17*, No. 100260.
(51) Jin, A.; Bennie, R. Z.; Ogilvie, O. J.; Trlin, H. J. F.; Kong, N. S.; Yu, H.; Dobson, R. C. J.; Domigan, L. J. Sculpting the Future of Meat: Biomaterial Approaches and Structural Engineering for Large-Scale Cell-Based Production. *Sustainable Food Proteins* **2024**, *2* (1), 3−20.
(52) Jongpaiboonkit, L.; King, W. J.; Lyons, G. E.; Paguirigan, A. L.; Warrick, J. W.; Beebe, D. J.; Murphy, W. L. An Adaptable Hydrogel Array Format for 3-Dimensional Cell Culture and Analysis. *Biomaterials* **2008**, *29* (23), 3346−3356.
(53) Chen, X.; Foote, A.; Thibeault, S. L. Cell Density, DMSO Concentration and Needle Gauge Affect Hydrogel-Induced BM-MSC Viability. *Cytotherapy* **2017**, *19* (12), 1522−1528.
(54) Aamodt, J. M.; Grainger, D. W. Extracellular Matrix-Based Biomaterial Scaffolds and the Host Response. *Biomaterials* **2016**, *86*, 68−82.
(55) Sivaraj, D.; Chen, K.; Chattopadhyay, A.; Henn, D.; Wu, W.; Noishiki, C.; Magbual, N. J.; Mittal, S.; Mermin-Bunnell, A. M.; Bonham, C. A.; Trotsyuk, A. A.; Barrera, J. A.; Padmanabhan, J.; Januszyk, M.; Gurtner, G. C. Hydrogel Scaffolds to Deliver Cell Therapies for Wound Healing. *Front. Bioeng. Biotechnol.* **2021**, *9*, No. 660145.
(56) Helary, C.; Zarka, M.; Giraud-Guille, M. M. Fibroblasts within Concentrated Collagen Hydrogels Favour Chronic Skin Wound Healing. *J. Tissue Eng. Regener. Med.* **2012**, *6* (3), 225−237.
(57) Chang, P.; Guo, B.; Hui, Q.; Liu, X.; Tao, K. A Bioartificial Dermal Regeneration Template Promotes Skin Cell Proliferation in Vitro and Enhances Large Skin Wound Healing in Vivo. *Oncotarget* **2017**, *8* (15), 25226−25241.
(58) Cao, L.; Zhang, Z.; Yuan, D.; Yu, M.; Min, J. Tissue Engineering Applications of Recombinant Human Collagen: A Review of Recent Progress. *Front. Bioeng. Biotechnol.* **2024**, *12*, No. 1358246, DOI: 10.3389/fbioe.2024.1358246.
(59) Xu, Q.; Torres, J. E.; Hakim, M.; Babiak, P. M.; Pal, P.; Battistoni, C. M.; Nguyen, M.; Panitch, A.; Solorio, L.; Liu, J. C. Collagen- and Hyaluronic Acid-Based Hydrogels and Their Biomedical Applications. *Mater. Sci. Eng. R Rep.* **2021**, *146*, No. 100641.
(60) Reiss, J.; Robertson, S.; Suzuki, M. Cell Sources for Cultivated Meat: Applications and Considerations throughout the Production Workflow. *Int. J. Mol. Sci.* **2021**, *22* (14), No. 7513.
(61) Wang, T.; Lew, J.; Premkumar, J.; Poh, C. L.; Naing, M. W. Production of Recombinant Collagen: State of the Art and Challenges. *Eng. Biol.* **2017**, *1* (1), 18−23.

https://doi.org/10.1021/acsbiomaterials.5c02203
ACS Biomater. Sci. Eng. 2026, 12, 3177−3187